

Mapping the Fluorescence Performance of a Photochromic–Fluorescent System Coupled with Gold Nanoparticles at the Single-Molecule–Single-Particle Level

Sabrina Simoncelli,^{†,‡,§} M. Julia Roberti,^{†,‡,§,||} Beatriz Araoz,^{‡,§} Mariano L. Bossi,^{‡,§} and Pedro F. Aramendía^{*,†,§}

[†]Centro de Investigaciones en Bionanociencias (CIBION-CONICET), Godoy Cruz 2390, 1425 Buenos Aires, Argentina

[‡]Instituto de Química Física de Materiales, Ambiente y Energía, (INQUIMAE-CONICET), Pabellón 2, Ciudad Universitaria, 1428 Buenos Aires, Argentina

[§]Departamento de Química Inorgánica, Analítica y Química Física, Facultad de Ciencias Exactas y Naturales, Universidad de Buenos Aires, Pabellón 2, Ciudad Universitaria, 1428 Buenos Aires, Argentina

Supporting Information

ABSTRACT: Single-molecule (SM) fluorescence microscopy was used to investigate the photochromic fluorescent system spiropyran–merocyanine (SP ↔ MC) interacting with gold nanoparticles (AuNPs). We observe a significant increase in the brightness of the emissive MC form, in the duration of its ON time, and in the total number of emitted photons. The spatial distribution of SMs with improved photophysical performance was obtained with 40 nm precision relative to the nearest AuNP. We demonstrate that even photochromic systems with poor photochemical performance for SM can become suitable for long time monitoring and high performance microscopy by interaction with metallic NP.

The interaction of the plasmonic resonant band of gold nanoparticles (AuNPs) with electronic states of nearby molecules has been extensively studied not only for a fundamental understanding but also for its practical implications.^{1,2} The proximity of an electronically excited molecule to a metallic nanostructure results in a deeply modified molecular photophysical behavior,³ through resonant coupling of the electronic transitions of both parties. This effect operates at characteristic distances on the order of the nanostructure size, and it is strongly dependent on the chromophore–surface distance, the overlap between the plasmon and the molecular transition bands (absorption and emission), the orientation of the molecular transition moment, and the molecular fluorescence emission quantum yield.⁴ This results in an increase in the rate of excited state production, as well as in the rates of radiative and nonradiative deactivation of the excited state. The latter two cause a decrease in the excited state lifetime, but the complex interplay between the distance dependence of the intervening processes may result in an increase or a decrease in the brightness of the molecule, depending on which process prevails at a certain position.^{1,3} In addition, an increase in the fluorophore photostability may be observed.^{4b} This AuNP–fluorophore interaction is particularly appealing in the development of molecular sensors and fluorescent probes for far-field microscopies, which strongly

benefit from the resulting effects of a lower detection limit and a higher resistance to photodamage that allows imaging molecules for longer periods of time.⁵

In recent years there has been renewed interest in the design of improved fluorescent optical switches or systems with activatable fluorescence with high brightness, low fatigue, and high switching reliability,⁶ led by novel concepts in far-field microscopy with subdiffraction resolution. These approaches rely on molecular systems with two stable or one metastable state with highly different emission features.⁷ In this regard, photochromic systems are of particular interest because of their versatility and the fact that they allow the lowest levels of irradiation power.⁸

Here, we use metallic nanostructures to improve the performance of a photochromic fluorescent system at the single-molecule (SM) level, focusing in three key aspects: (i) enhance the brightness (B) of the emissive isomer, (ii) increase the average ON time of the fluorescent isomer (τ_{ON} , by decrease of the photobleaching efficiency), and (iii) increase the total number of photons emitted before photobleaching (N_{PH}). We use well-known spiropyran–merocyanine isomers to quantify the interaction of AuNPs with single photochromic molecules. This is achieved by statistical analysis of SM time traces with high-resolution optical localization of them in the neighborhood of the metallic surface and comparing them with the performance of a control system in the absence of AuNPs. AuNPs were chosen because of their photo and thermal stability, their low chemical reactivity, and the plasmonic band located in the center of the visible spectrum (ca. 532 nm for spherical structures of up to 100 nm diameter). The selected photochrome, 1,3',3'-trimethyl-6-nitrospiro-[2H-1-benzopyran-2,2'-indoline] (SP), displays reliable and well characterized thermal and photo interconversion between isomers.⁹ The cleavage of a C–O bond of the spirobenzopyran ring leads to the merocyanine (MC) form with an absorption band centered at 550 nm, with a considerable overlap with the plasmonic band of the spherical AuNPs used in this work, thus allowing for

Received: March 13, 2014

Published: April 25, 2014

enhancement of the weak MC red fluorescence (Figure S1A). Spherical AuNPs of 68 ± 3 nm in diameter (Figure S1B) were prepared by the seed-mediated growth method,¹⁰ and fixed to organo-silanized glass substrates. The samples were finally covered by spin coating a poly(propyl methacrylate) (PPMA) film of nanometer thickness, containing SP dye (10^{-3} mol/kg polymer). The films were characterized by profilometry and AFM (Figure S2).

Temporal sequences of fluorescence images were obtained in a wide-field microscope irradiating the sample with 532 nm linearly polarized light (see Supporting Information (SI) Section 5). Spontaneous thermal ring-opening of SP to MC sufficed to induce a reasonable frequency of ON events. Analysis of SM time traces was performed with homemade MATLAB routines (SI Section 7) to obtain the dynamics of MC single molecules (B , τ_{ON} , and N_{PH}), as well as the relative distance of each molecule with respect to the nearest NP with nanometric localization precision.

Single-molecule detection was ensured by the low number of activated MC molecules in the field of view (i.e., average distance between emitter spots larger than a point spread function, PSF) as well as by the one step ON-OFF behavior of the emission traces (SI Sections 6–8). First, we made a statistical analysis of B , τ_{ON} , and N_{PH} distribution of single MC molecules detected in PPMA films in the absence of AuNPs. Afterward, we repeated the same measurements but in films deposited on cover glasses where AuNPs were attached. In these latter cases, we restricted our detection analysis to MC molecules turned ON in an area of 780×780 nm² around a detected AuNP. This area, multiplied by the sample thickness, includes in the sample a volume considerably larger than the volume of a 68 nm diameter AuNP plus the volume of the enhanced electric field region (SI Section 6). This latter region, originated on the plasmon interaction with light, can be estimated as a cylinder of 20 nm radius and 10 nm thickness extending at both sides of the nanostructure in the direction of the light polarization direction.¹¹ Therefore, many SM traces selected in this way would resemble those traces of molecules either far from NPs or belonging to films without AuNPs. Owing to this low probability, we decided to use the complementary cumulative distribution function (CCDF)¹² to perform the quantitative analysis of SM data. The value of the CCDF, $\Phi_C(x)$, is related to the integral of the probability distribution function ($f(x)$) by

$$\Phi_C(x) = P(X > x) = \int_x^\infty f(x) dx \quad (1)$$

The CCDF is the probability, P , that a random variable, x , can have a value above a particular level, X , i.e., $P(X > x)$. Figure 1 displays the results obtained for the CCDF of B (panel A), N_{PH} (panel B), and τ_{ON} (panel C) for MC molecules switching ON in the absence of AuNPs (red) and in the vicinity of single AuNPs (blue). A clear difference in the photophysics of these two ensembles is observed. MC molecules in the presence of AuNP exhibit higher probability of longer ON times and higher brightness compared to isolated molecules. The increase in these two parameters results in a higher N_{PH} , with a higher contribution from the increase in τ_{ON} . On the other hand, considering that the thermal average time of MC molecules in poly(alkyl methacrylate) films near room temperature is in the range of minutes,¹³ the ON times in the seconds range observed in these experiments are determined by photobleaching. Thus, the longer τ_{ON} reflect a lower photobleaching

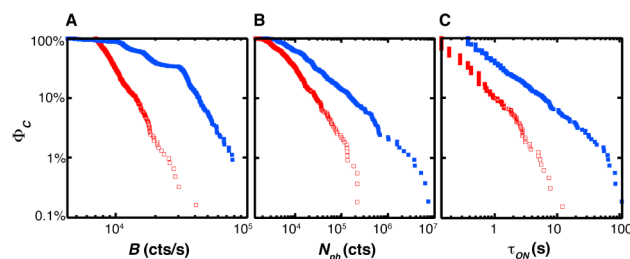


Figure 1. Φ_C for B (A), N_{PH} (B), and τ_{ON} (C) of MC single molecules embedded in PPMA thin films of 23 ± 3 nm thickness detected over 68 nm diameter AuNPs (blue). Similar data collected in the absence of AuNPs (red) are also shown.

probability. This is due to the excited state lifetime decrease of MC fluorescent molecules through radiative and nonradiative rate enhancement by the AuNP plasmonic interaction.^{1,3} The higher N_{PH} is essential to increase the accuracy in localization of the position of the fluorescent molecule with subdiffraction limited precision, whereas the longer average τ_{ON} widens the time window to monitor dynamic processes by SM spectroscopy.

The plots of Figure 1 do not display the spatial information on the molecules correlated to their τ_{ON} . To show this relation, we concentrate in molecules displaying $\tau_{\text{ON}} > 5$ s. Considering that the average τ_{ON} of MC molecules in the absence of AuNP is 0.5 s, the considered ensemble shows more than 10 times more photostability than the average MC molecule far away from a AuNP. Furthermore, in view of the results displayed in Figure 1, less than 1% of the MC ON events are above this threshold in the absence of AuNP, compared to around 10% of the detected molecules in the vicinity of a AuNP. The position of this molecular ensemble and the distance to the corresponding AuNP was determined with ca. 40 nm uncertainty. This information is displayed in Figure 2. The distribution of the $\tau_{\text{ON}} > 5$ s molecules clusters in the direction of the incident light polarization at each side of the generic AuNP (which is located in the center of the image). No molecule of this ensemble is located at a distance greater than

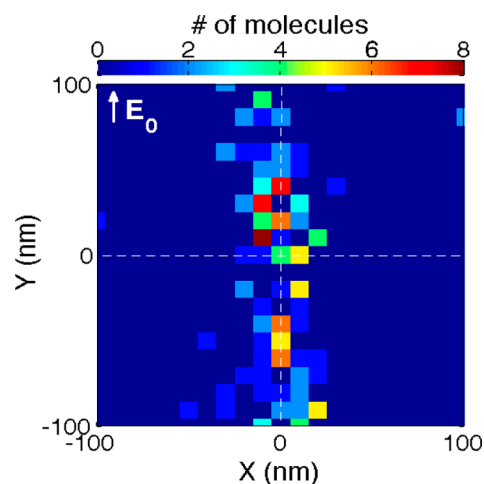


Figure 2. Super resolution localization of MC single molecules detected over a single AuNP (2D-histogram, 10×10 nm² bins). Their position is referred to the nearest AuNP in the image field. The histogram was constructed with all the MC molecules that displayed $\tau_{\text{ON}} > 5$ s (data from all the different film thicknesses). The laser polarization direction is along the y -axis.

100 nm from the center of the nearest AuNP. All these facts are consistent with the expected distribution of the enhanced electric field and its consequence on photophysical properties of fluorescent molecules. As expected,¹⁴ two maxima at each side of the NP can be outlined. The distance between maxima in the figure is ca. 50 nm, smaller than the expected value of ca. 80 nm for 68 nm diameter AuNP, but within the experimental uncertainty of the experiment.¹⁵

We demonstrated that with one color experiment we were able to increase the brightness, the ON time, and the total number of detected photons for single-molecule imaging of a fluorescent photochromic system. Particularly, the improvement in N_{PH} allowed super localization of the individual molecules and the correlation between location and improved photophysical performance. Our approach demonstrates that even with photochromic systems that display poor photochemical performance for SM spectroscopy and superlocalization, the use of the plasmonic interaction can turn them useful for long time monitoring and nanometric localization, suitable for high performance microscopy.

■ ASSOCIATED CONTENT

📄 Supporting Information

Gold nanoparticle synthesis details, slides surface modification, AuNP coating, polymer film preparation and characterization, and SM time traces analysis. This material is available free of charge via the Internet at <http://pubs.acs.org>.

■ AUTHOR INFORMATION

Corresponding Author

pedro.aramendia@cibion.conicet.gov.ar

Present Address

^{||}M.J.R.: European Molecular Biology Laboratory. EMBL. Heidelberg. Germany.

Notes

The authors declare no competing financial interest.

■ ACKNOWLEDGMENTS

P.F.A. and M.L.B. are Research Staff from CONICET. S.S., M.J.R., and B.A. held research fellowships from CONICET. Financial support from UBA (Grant 20020100100234) and CONICET (Grant 11220100100397) is acknowledged.

■ REFERENCES

- (1) (a) Anger, P.; Bharadwaj, P.; Novotny, L. *Phys. Rev. Lett.* **2006**, *96*, 113002. (b) Lakowicz, J. R. *Anal. Biochem.* **2001**, *298*, 1–24. (c) Gersten, J.; Nitzan, A. *J. Chem. Phys.* **1981**, *75*, 1139–1152.
- (2) Darvill, D.; Centeno, A.; Xie, F. *Phys. Chem. Chem. Phys.* **2013**, *15*, 15709–15726.
- (3) (a) Gosh, S. K.; Pal, T. *Phys. Chem. Chem. Phys.* **2009**, *11*, 3831–3844. (b) Bharadwaj, P.; Novotny, L. *Opt. Express* **2007**, *15*, 14266–14274.
- (4) (a) Guerrero, A. R.; Aroca, R. F. *Angew. Chem., Int. Ed.* **2011**, *50*, 665–668. (b) Estrada, L. C.; Roberti, M. J.; Simoncelli, S.; Levi, V.; Aramendía, P. F.; Martínez, O. E. *J. Phys. Chem. B* **2012**, *116*, 2306–2313.
- (5) (a) Jain, P. K.; Huang, X.; El-Sayed, I. H.; El-Sayed, M. A. *Acc. Chem. Res.* **2008**, *41*, 1578–1586. (b) Aslan, K.; Lakowicz, J. R.; Geddes, C. D. *Curr. Opin. Chem. Biol.* **2005**, *9*, 538–544.
- (6) Hell, S. W. *Nat. Methods* **2009**, *6*, 24–32.
- (7) Montenegro, H.; Di Paolo, M.; Capdevila, D.; Aramendía, P. F.; Bossi, M. L. *Photochem. Photobiol. Sci.* **2012**, *11*, 1081–1086.
- (8) (a) Deniz, E.; Tomasulo, M.; Cusido, J.; Yildiz, I.; Petriella, M.; Bossi, M. L.; Sortino, S.; Raymo, F. M. *J. Phys. Chem. C* **2012**, *116*,

6058–6068. (b) Fukaminato, T. *J. Photochem. Photobiol., C* **2011**, *12*, 177–208. (c) Shu, X.; Royant, A.; Lin, M. Z.; Aguilera, T. A.; Lev-Ram, V.; Steinbach, P. A.; Tsien, R. Y. *Science* **2009**, *324*, 804–807.

(9) Bertelson, R. C. Spiropyrans. In *Organic Photochromic and Thermochromic Compounds*; Crano, J. C., Guglielmetti, R. J., Eds.; Kluwer Academic/Plenum Publishers: New York, 1999; Vol. 1, Main Photochromic Families.

(10) Niu, J.; Zhu, T.; Liu, Z. *Nanotechnology* **2007**, *18*, 325607.

(11) (a) Novotny, L.; Hecht, B. *Principles of Nano-Optics*; Cambridge University Press: New York, 2006. (b) Estrada, L. C.; Aramendía, P. F.; Martínez, O. E. *Opt. Express* **2008**, *16*, 20597–20602. (c) Encina, E. R.; Coronado, E. A. *J. Phys. Chem. C* **2007**, *111*, 16796–16801.

(12) Hellriegel, C.; Kirstein, J.; Bräuchle, C.; Latour, V.; Pigot, T.; Olivier, R.; Lacombe, S.; Brown, R.; Guieu, V.; Payaraste, T.; Izquierdo, A.; Mocho, P. *J. Phys. Chem. B* **2004**, *108*, 14699–14709.

(13) Levitus, M.; Talhavini, M.; Negri, R. M.; Zambon Atvars, T. D.; Aramendía, P. F. *J. Phys. Chem. B* **1997**, *101*, 7680–7686.

(14) The higher detected molecular density does not represent directly the spatial distribution of the enhanced electric field but is a result of the effects in the photophysical properties, namely, B , τ_{ON} , and N_{PH} , that improve the detectability of the molecules.

(15) The localization uncertainty strongly depends on the number of detected photons. Typically, in these experiments, it is between 9 and 40 nm.